Aliphatic carbonyl reduction promoted by palladium catalysts under mild conditions

Maria Grazia Musolino [a], Concetta Busacca [a], Francesco Mauriello [b], Rosario Pietropaolo [a,*]

[a] Dipartimento di Meccanica e Materiali, Facoltà di Ingegneria, Università Mediterranea di Reggio Calabria, Loc. Feo di Vito, I-89122 Reggio Calabria, Italy
[b] Dipartimento di Scienza dei materiali e Ingegneria Chimica, Politecnico di Torino, Corso Duca degli Abruzzi, 24-10129 Torino, Italy

ARTICLE INFO

ABSTRACT

The catalytic reduction of aliphatic aldehydes (propanal, pentanal and hexanal) and ketones (pentan-2-one, pentan-3-one and cyclohexanone) to the corresponding alcohols promoted by palladium catalysts, such as Pd/CoO, Pd/NiO, Pd/ZnO, Pd/Fe$_2$O$_3$ and Pd/CeO$_2$, was performed under mild conditions (0.1 MPa H$_2$ and 323 K) for the first time.

All the catalysts were obtained by the co-precipitation technique and characterized by BET, TPR, XRD, TEM and XPS. The co-precipitation method allows, after reduction, formation of bimetallic ensembles (Pd/CoO and Pd/ZnO in less extent) or alloys (Pd/NiO) thus changing the electronic properties of the palladium on the surface, increasing the d-orbital energy at the Fermi level and permitting the activation of the C=O bond also in aliphatic carbonyls. Accordingly the reactivity of Pd/Fe$_2$O$_3$ and Pd/CeO$_2$ towards aliphatic aldehydes is attributed to a redox interaction of Fe^{3+} or Ce^{4+} with the oxygen moiety of the carbonyl bond, leading to the π* orbital energy decrease.

Analogous reactions, carried out with Pd/CoO and Pd/Fe$_2$O$_3$, prepared by impregnation, gave a very slow reduction.

Additional catalytic tests were performed with aromatic carbonylic compounds in order to compare their reactivity with that of aliphatic systems: the differences were interpreted taking into account the Δ energy value between π and π* orbitals, much lower in aromatic carbonyls, that favours an easier activation of the aromatic C=O bond.

© 2010 Elsevier B.V. All rights reserved.

1. Introduction

The reduction of carbonyl compounds generally occurs through two different pathways: (i) nucleophilic addition of a hydride ion to the electrophilic carbon atom of a carbonyl molecule, followed by a fast proton attack on the transient anion and (ii) stepwise addition of activated hydrogen atoms to a metal bonded C=O group. The first one implies the use of NaBH$_4$ or LiAlH$_4$, as hydride source, and the driving force of the reaction rests on the different electronegativity between carbon and oxygen. The second involves an attack of a weak nucleophile such as the metal bonded hydrogen on a suitable empty orbital located on the carbonyl carbon. Generally, transition metals, such as Pt, Ru and Rh, hydrogenate both C=C and C=O double bonds and Os and Ir are the most active catalysts towards the C=O hydrogenation [1–4]. Furthermore both alloys, formed by platinum group metals associated with electropositive metal atoms [5–7] or oxidated metal species (Sn^{2+}, Fe^{2+}, Fe^{3+}, Ge^{4+}) on a surface of a noble metal, acting as Lewis acids, may promote activation of the C=O bond "via" the lone pair of oxygen. The involved mechanism, generally referred as "electrophilic C=O activation" was most frequently invoked to account for the promoting effect of electropositive ions [8–10].

No similar effect was, so far, reported for palladium systems in mild conditions. As far as we know the only hydrogenation reaction of aliphatic carbonyl compounds was reported to occur at 1 MPa H$_2$ pressure, ten times higher than that normally used in mild conditions [11]. To interpret this behaviour two different explanations were reported: Delbecq and Sautet [12] remark that the lower value of the radial "d" function, compared with that of other metals, in Pd systems, reduces the activation of the carbonyl bond; conversely, Ponec and Bond mention that the weakness of adsorption through the carbonyl group could be, in turn, caused by the change in electronic structure of palladium surface atoms ($4d^{9,7}5s^{0,3} \rightarrow 4d^{10}5s^0$) induced by hydrogen atoms in interstitial positions [13]. The problem is indeed further complicated if we take into account that aromatic aldehydes are easily hydrogenated by common palladium catalysts [14,15]. Hydrogen transfer reactions from alcohols to aromatic carbonyls promoted by palladium samples were also reported [16,17].

* Corresponding author. Tel.: +39 0965 875256; fax: +39 0965 875248.
E-mail address: rosario.pietropaolo@unirc.it (R. Pietropaolo).

Table 1
Main characteristics of supported Pd catalysts.

Catalyst code	Support	Palladium loading (wt%)		S.A. (m²/g)	d_n (nm)[a]
		Nominal	XRF		
PdCo	CoO	5	3.7	106	10.7
PdNi	NiO	5	5.0	90	4.2
PdZn	ZnO	5	5.2	85	2.7
PdFe	Fe₂O₃	5	8.7	170	2.4
PdCe	CeO₂	5	4.9	15	–
PdCoI[b]	CoO	5	4.5	8	4.3
PdFeI[b]	Fe₂O₃	5	5.5	6	7.1

[a] Mean particles size from TEM.
[b] Catalysts prepared by the impregnation technique.

On this basis it seems that the lack of activity so far observed with supported palladium systems, in hydrogenation of aliphatic carbonyl groups, has to be mainly attributed to electronic factors involving both the metal and the organic C=O moiety. Therefore, in principle, it may be possible to achieve a different chemical deal modifying the electronic properties of palladium by using a better fitting support and a suitable catalyst method preparation.

Indeed, some of the authors have recently published on the selective hydrogenation of campholenic aldehyde to naturanol promoted by palladium catalysts [18,19], with an essential industrial purpose; however, the fundamental chemical reasons disfavouring the C=O hydrogenation with palladium systems are still lacking. With this aim we report in this paper on the catalytic performance of supported palladium catalysts, obtained by the co-precipitation technique (Pd/CoO, Pd/NiO, Pd/ZnO, Pd/Fe₂O₃ and Pd/CeO₂), in the reduction of some carbonyl compounds.

For comparison analogous reactions have been carried out with Pd/CoO and Pd/Fe₂O₃, prepared by the impregnation technique.

A characterization of the structural properties of the catalysts used by nitrogen adsorption (BET), X-ray diffraction (XRD), temperature-programmed reduction (TPR), X-ray photoelectron spectroscopy (XPS), transmission electron microscopy (TEM) was also performed with the aim to link the observed reactivity to the structure of the catalysts.

2. Experimental

2.1. Catalysts preparation

All catalysts, with a nominal palladium loading of 5 wt%, were prepared by the co-precipitation technique from aqueous solutions of the corresponding inorganic precursors, palladium chloride anhydrous (Fluka, purity 60% Pd) dissolved in HCl, poured with cobalt(II) nitrate hexahydrate (Fluka, purity ≥99%), nickel(II) nitrate hexahydrate (Aldrich, purity 98%), zinc(II) nitrate hexahydrate (Aldrich, purity 98%), iron(III) nitrate nonahydrate (Fluka, purity ≥98%) or cerium(III) nitrate hexahydrate (Aldrich, purity ≥99%). The so-obtained aqueous metal salt solutions were added, drop by drop, into an aqueous solution of Na₂CO₃ 1 M. After filtration and washing until chloride was removed, samples were dried for 1 day under vacuum at 353 K and further reduced at 473 K for 2 h under flowing hydrogen. Only the Pd/CeO₂ catalyst was calcined at 773 K for 5 h before reduction.

In the Pd/CoO specimen, formation of small Co particles makes it unstable when exposed to air. Therefore, it was managed, after the reduction treatment, avoiding, as much as possible, contact with air.

5% palladium catalysts were also prepared by incipient wetness impregnation of the commercial supports CoO (Aldrich, S_{BET} = 7 m²/g) and Fe₂O₃ (Sigma–Aldrich, S_{BET} = 4 m²/g) with an acetone solution of palladium(II) acetylacetonate (Aldrich, purity 99%). After impregnation the samples were dried for 1 day under vac-

uum at 353 K and further reduced at 473 K for 2 h under flowing hydrogen. The main characteristics of the catalysts are reported in Table 1.

2.2. Catalysts characterization

Temperature-programmed reduction (TPR) measurements were performed using a conventional TPR apparatus. The dried samples (50 mg) were heated at a linear rate of 10 K/min from 298 to 1273 K in a 5 vol.% H₂/Ar mixture at a flow rate of 20 cm³/min. H₂ consumption was monitored by a thermal conductivity detector (TCD). A molecular sieve cold trap (maintained at 193 K) and a tube filled with KOH, placed before the TCD, were used to block water and CO₂, respectively. The calibration of signals was made by injecting into the carrier a known amount of H₂.

BET surface area was determined by N₂ adsorption–desorption isotherms at liquid nitrogen temperature by using a Micromeritics Chemisorb 2750 instrument. The composition of the flow gas was N₂:He = 30:70. Samples were outgassed under flowing nitrogen for 1 h at 473 K, prior to measurements.

The catalyst particle size and the relative morphology were analyzed by transmission electron microscopy (TEM), using a JEOL 2000 FX instrument operating at 200 kV and directly interfaced with a computer for real-time image processing. The specimens were prepared by grinding the powder reduced catalyst in an agate mortar, then suspended in isopropanol. A drop of the suspension, previously dispersed in an ultrasonic bath, was deposited on a copper grid coated by a holey carbon film. After evaporation of the solvent, the specimens were introduced into the microscope column. Particle size distributions were obtained by counting several hundred particles visible on the micrographs on each sample. From the size distribution the number average diameter was calculated: $d_n = \sum n_i d_i / \sum n_i$ where n_i is the number of particles of diameter d_i.

Powder X-ray diffraction (XRD) data were acquired at room temperature on a Philips X-Pert diffractometer, by using the Ni β-filtered Cu Kα radiation (λ = 0.15418 nm). Analyses were performed on reduced samples at 473 K for 2 h and registered in the 2θ range of 5–80° at a scan speed of 0.5°/min. Diffraction peaks were compared with those of standard compounds reported in the JPCDS Data File.

X-ray photoelectron spectroscopy (XPS) analysis was performed on fresh and reduced, at 473 K for 2 h, samples, by using a Physical Electronics GMBH PHI 5800-01 spectrometer, equipped with a monochromatic Al Kα X-ray source. The binding energy was calibrated taking the C 1s peak (284.8 eV) as reference.

2.3. Catalytic tests

Liquid phase hydrogenation of aliphatic and aromatic aldehydes (propanal, pentanal, hexanal, 3-phenylpropanal and benzaldehyde) and ketones (pentan-2-one, pentan-3-one, cyclohexanone and 1-phenylethanone) was carried out at 0.1 MPa partial hydro-
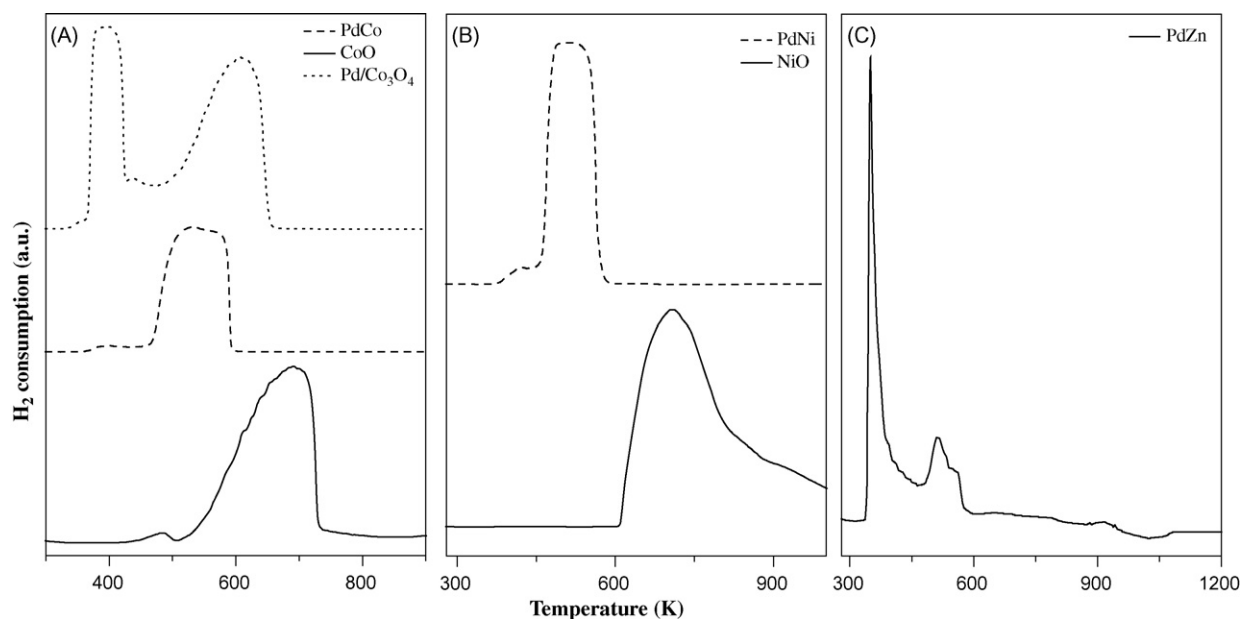
Fig. 1. H_2-TPR profiles of CoO, NiO and ZnO supported palladium catalysts and of the CoO and NiO supports.

gen pressure in a 100 ml five-necked batch reactor fitted with a reflux condenser. The reaction temperature was maintained at a constant value (323 K) by circulation of silicone oil in an external jacket connected with a thermostat. The temperature of the reaction mixture was monitored by placing a thermocouple inside the vessel. A typical run was carried out as follows. The catalyst (about 300 mg), previously activated under H_2 at 473 K, was added to the required amount of solvent (25 ml of ethanol - Fluka, 99.8% analytical grade), and further reduced in "situ" at 323 K for 1 h under H_2 flow (50 ml/min). Then, a solution of a carbonyl compound in ethanol (0.6 M, 15 ml), containing tetradecane as internal standard, was added through one arm of the flask. The reaction mixture was stirred with a magnetic stirrer head coupled with a gas stirrer at a rate of 500 rpm.

Preliminary runs, performed with different amounts of catalyst, sample grain size and stirring rate, indicated that, under the experimental conditions adopted, the reaction was carried out in absence of external and internal mass-transfer limitations.

The progress of the reaction was followed by analyzing a sufficient number of samples withdrawn periodically from the reaction mixture. Products analysis was performed with a gas chromatograph (HP model 5890), equipped with a wide-bore capillary column (CP-WAX 52 CB, 50 m, i.d. = 0.53 mm) and a flame ionization detector. Quantitative analysis was carried out by calculating the areas of the chromatographic peaks with an electronic integrator (HP model 3396).

3. Results

3.1. Catalysts characterization

3.1.1. Chemical composition and surface area determination

Table 1 reports the real wt% of the metal and the values of surface areas found on everyone of the catalysts used. The exact amount of Pd on our supports was determined by X-ray fluorescence (XRF) analysis. The surface areas of the co-precipitated catalysts change within a wide range (from 15 to 170 m²/g). However, the lowest BET area value (15 m²/g) found for PdCe is due to the calcination treatment performed. Also the PdCo sample, calcined at 773 K for 5 h, shows a remarkable decrease of the surface area (50 m²/g) with respect to the uncalcined (106 m²/g).

BET area values drastically decrease in the PdCoI and PdFeI samples, prepared by impregnation, having a surface area similar to that of the parent support.

3.1.2. Temperature-programmed reduction (TPR) measurements

Fig. 1 refers to the TPR profiles of co-precipitated palladium catalysts supported on CoO, NiO and ZnO. The profile of the fresh Pd/CoO sample shows a broad and intense peak centered at ∼535 K including both palladium and cobalt simultaneously reduced. Interestingly, no negative peak, attributable to β-hydride decomposition, is observed. For a comparison the TPR spectrum of a pure CoO sample is also included in Fig. 1A and a reduction interval ∼550–790 K was observed. Indeed PdCo supported catalysts were, so far, abundantly studied [20–22] and some interesting structural evidences may be actually taken into account. In systems, containing both PdO and Co_3O_4 supported oxides, after calcination in air and subsequent H_2 reduction, the main peculiarities appear to be: (i) palladium and cobalt oxides are in intimate contact already in the precursor state; (ii) there is a strong promoting effect of palladium on cobalt oxide reduction also at low temperatures; (iii) TPR experiments coupled with EDX analysis and magnetic measurements confirm that particles contain both metals and EXAFS spectra emphasize the presence of alloys; the absence of any H_2 desorption confirms the result; (iv) XANES spectra favour the presence of alloys suggesting also a shift of electrons from Co to Pd [21]. Taking into account the reported rich literature our results suggest that the H_2 reduction of the co-precipitated PdCo sample affords PdCo ensembles (possibly alloys) and Co. Furthermore the TPR carried out on the Pd/CoO sample, previously reduced at 473 K for 2 h, confirms the absence of any palladium β-hydride species on the bulk of the catalyst and also that all palladium has been totally reduced.

The TPR profile of the Pd/NiO catalyst (see Fig. 1B) is nearly identical to that of Pd/CoO, previously reported. The very broad and particularly intense peak, centered at 512 K, observed refers to the simultaneous reduction of both palladium and nickel cations, suggesting again that NiPd species are formed. No palladium β-hydride species both on the fresh and on the previously reduced sample were detected. All considerations, above reported for the PdCo intimate structure, can be reversed on formation of NiPd species. Again,
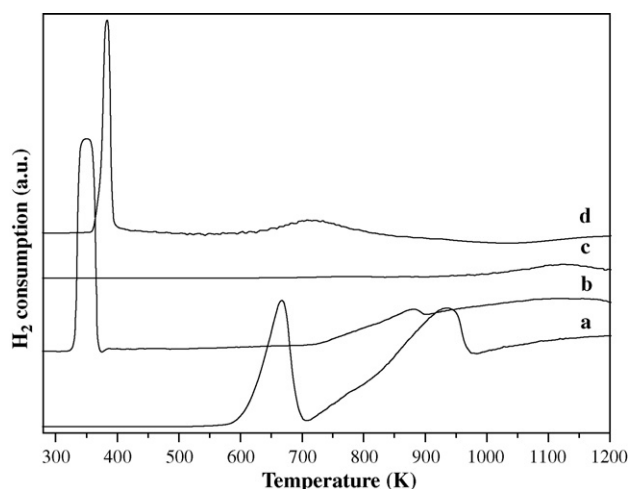
Fig. 2. H_2-TPR profiles of Fe_2O_3 and CeO_2 supported palladium catalysts and of the Fe_2O_3 and CeO_2 supports: (a) Fe_2O_3; (b) PdFe; (c) CeO_2; (d) PdCe.
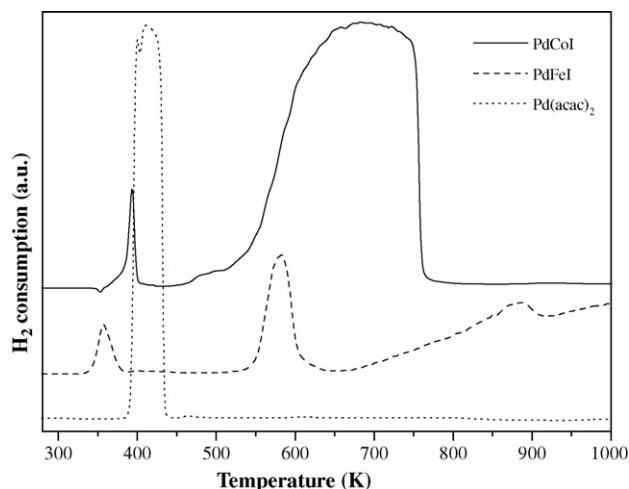

Fig. 3. H_2-TPR profiles of CoO and Fe_2O_3 supported palladium catalysts, prepared by impregnation, and of the precursor $Pd(acac)_2$.

for a comparison, the TPR of a pure sample of NiO was performed and a reduction interval ~635–850 K was observed (Fig. 1B).

Conversely, the TPR spectrum of palladium supported on cobalt oxide, after calcination at 773 K for 5 h, is totally different (Fig. 1A). H_2 uptake quantitative analysis, in fact, indicates that the peak centered at 394 K involves simultaneous reduction of $Pd^{2+} \rightarrow Pd^{\circ}$ and $Co(III) \rightarrow Co_3O_4$, the first being shifted at a higher temperature than that normally found for supported palladium catalysts [23]. Moreover, the very broad peak, centered at 608 K, belongs to the $Co_3O_4 \rightarrow CoO \rightarrow Co$ reduction. The TPR profile of Pd/ZnO (see Fig. 1C) shows the main peak centered at 352 K, ascribed to a palladium cation amount reduction of about 87%. The temperature value recalls that already reported for impregnated Pd/ZnO catalysts [24]. Another peak, small and broad, centered at 514 K, appears, unusually, on the spectrum. We attribute it to a simultaneous reduction of Pd^{2+} and Zn^{2+}, leading to a little amount (~13%) of PdZn particles. The H_2 moles involved allow this interpretation. As normally found, no further reduction was observed until 1273 K. No β-hydrides were detected both on the fresh and on the previously reduced at 473 K sample.

Fig. 2 reports, all together, TPR profiles relative to Fe_2O_3, Pd/Fe_2O_3, CeO_2 and Pd/CeO_2, with the aim of having a ready interpretation of the catalysts reduction peculiarities through a comparison of the supported palladium profiles with those of pure oxides. Indeed, for the co-precipitated Pd/Fe_2O_3 system, our work is facilitated since we take into account some results already published [25–27]. Beginning from the reduction profile of Fe_2O_3 (Fig. 2a) the peak at 694 K belongs to the reduction $Fe(III) \rightarrow Fe_3O_4$ and that at 963 K to the subsequent reduction $Fe_3O_4 \rightarrow FeO$, according to our H_2 consumption calculations. On the PdFe catalyst profile (Fig. 2b), the most interesting feature rests on the very large shift of the reduction temperature relative to the reaction $Fe(III) \rightarrow Fe_3O_4$ from 694 to 352 K, respectively determined in absence and in presence of Pd^{2+}. H_2 consumption calculations demonstrate very well, in fact, that the 352 K absorption area includes both $Pd(II) \rightarrow Pd(0)$ and $Fe(III) \rightarrow Fe_3O_4$ reductions. There is no doubt that reduction of palladium cations catalyzes that of $Fe(III)$ to the more stable magnetite but the temperature gap is too wide to be underlined. A similar effect was not found with Au/Fe_2O_3 or Ru/Fe_2O_3 systems [28,29]. The large availability of hydrogen atoms on the palladium surface is certainly responsible of the observed behaviour. The second peak at 882 K belongs to the $Fe_3O_4 \rightarrow FeO$ reduction. In this case the temperature shift is relatively small ($963 \rightarrow 882$ K) since the role of the reduced palladium is

less important. As far as the PdCe profile is concerned (Fig. 2d), the H_2 consumption area centered at 383 K is higher than that relative to the only $Pd^{2+} \rightarrow Pd^{\circ}$ reduction (2.4×10^{-5} moles of Pd^{2+} against 4.2×10^{-5} moles of H_2 consumed). Indeed a similar phenomenon was already observed and interpreted invoking a simultaneous reduction of both palladium cations and the small amount of CeO_2, interacting with it, forming Ce^{3+} ions [30,31]. The peak at 714 K should be attributed to interacting with Pd^{2+} surface CeO_2 particles reduction. No other peaks were detected. Fig. 3 includes TPR profiles of Pd/CoO and Pd/Fe_2O_3, prepared by impregnation, and, for comparison, of the precursor $Pd(acac)_2$. For both samples the first peak refers to the only $Pd^{2+} \rightarrow Pd^{\circ}$ reduction and is close to that of $Pd(acac)_2$. H_2 uptake quantitative analysis thoroughly supports this conclusion. The second peak attains, respectively, to $Co^{2+} \rightarrow Co^{\circ}$ and $Fe_2O_3 \rightarrow Fe_3O$ reduction and is weakly shifted towards lower temperatures with respect to that of pure oxides. Interestingly, β-hydride decomposition is observed at 359 K for PdCoI, indicating a scarce metal–support interaction. The main quantitative TPR results of catalysts are summarized in Table 2.

3.1.3. Transmission electron microscopy (TEM) measurements

Representative TEM microphotographs of the supported palladium catalysts, reduced at 473 K for 2 h, are shown in Fig. 4. The morphology of the matrix, on which metallic particles are distributed, is clearly characteristic of the support used. Moreover, on PdCo and PdNi it is possible to observe the presence of faceted metal particles, whereas on PdZn and PdFe palladium particles are distributed on the outer shell of the grains of the support. Based on the measurement of several hundred particles in random regions, the size distribution histograms have been obtained and displayed in Fig. 4 as an inset corner of the corresponding TEM image. The

Table 2
Quantitative results of H_2-TPR experiments.

Catalyst	H_2 consumption (μmol)[a]	Pd content (μmol)
PdCo	–	17.6
Pd/Co_3O_4 [b]	240	18
PdNi	–	23.6
PdZn	20	23
PdFe	117	40.7
PdCe	42	24
PdCoI	20	21.1
PdFeI	21	25.8

[a] At lower reduction temperature.
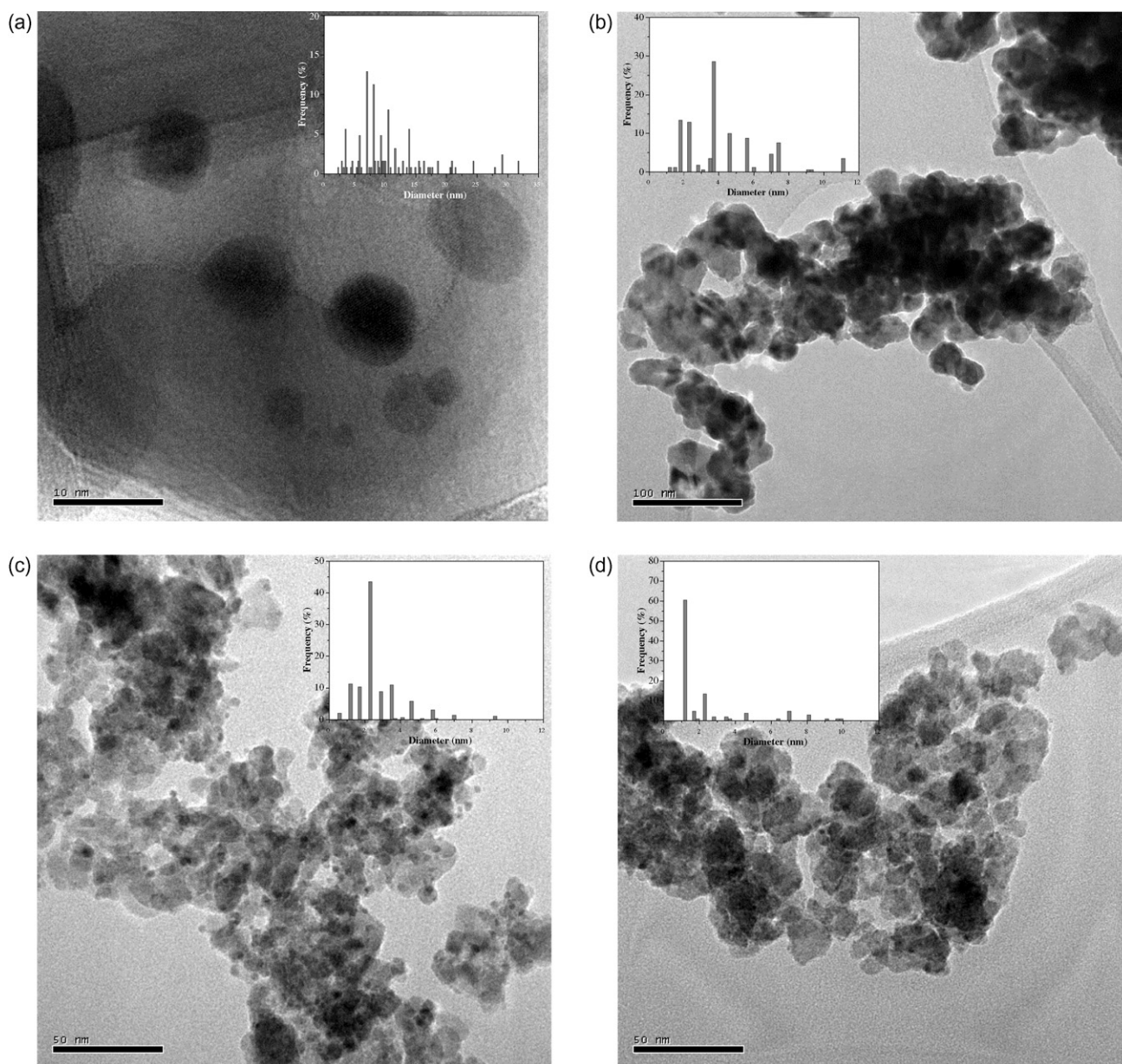[b] Calcined at 773 K.

Fig. 4. TEM microphotographs and metal particle size distribution histograms of different supported palladium catalysts: (a) PdCo; (b) PdNi; (c) PdZn; (d) PdFe.

average metallic particles diameter is reported in Table 1. The PdNi, PdFe and PdZn samples exhibit a predominance of small metallic particles and a relatively narrow particles size distribution. Conversely the PdCo catalyst shows a broad size distribution with a mean diameter of 10.7 nm, higher than the other samples. On the PdCe system the contrast between the metal particles and the matrix is not good enough to measure a large number of particles. Therefore, in this case, a true reliable distribution cannot be given.

TEM microphotographs of CoO and Fe_2O_3 supported palladium catalysts, prepared by impregnation, exhibit Pd particles dispersed on the matrix but also particles agglomeration spots. Moreover on the PdCoI sample a narrow particle size distribution centered around 4 nm is obtained, whereas on PdFeI particles in the range of 4–20 nm have been imaged.

3.1.4. Powder X-ray diffraction (XRD) analysis

Fig. 5 includes XRD spectra belonging to co-precipitated cobalt oxide supported palladium samples and a commercial CoO. In par-

ticular, spectra "b" and "c" attain to Pd/cobalt oxide specimens: the "b" one refers to Pd/cobalt oxide calcined at 773 K and reduced at 473 K, whereas "c" belongs to Pd/CoO used and then filtered at the end of a carbonyl compound hydrogenation reaction. Diffraction patterns observed on spectrum "b" are those belonging to Co_3O_4 and Pd [32–34]. Therefore, the above reported reduced supported sample should be correctly formulated as Pd/Co_3O_4. Conversely patterns of spectrum "c" attain to a hexagonal cobalt structure [34,35]. Fig. 6 belongs to both reduced Pd/NiO and Pd/ZnO catalysts. Peaks referring to NiO and, after deconvolution analysis, to both Ni and an alloy Pd(0.08)Ni(0.92) (Fig. 6a), ZnO and a broad palladium signal (Fig. 6b) are detected. Fig. 7 includes XRD spectra related to PdFe and PdCe samples after reduction with H_2 at 473 K. Patterns of the PdFe sample evidence only the magnetite structure, whereas Pd/CeO_2 signals attain to that of cerianite. The XRD spectra of PdCoI and PdFeI catalysts, prepared by impregnation, are reported in Fig. 8. Diffraction patterns observed reveal the presence of both palladium and the corresponding support structure (CoO and haematite).
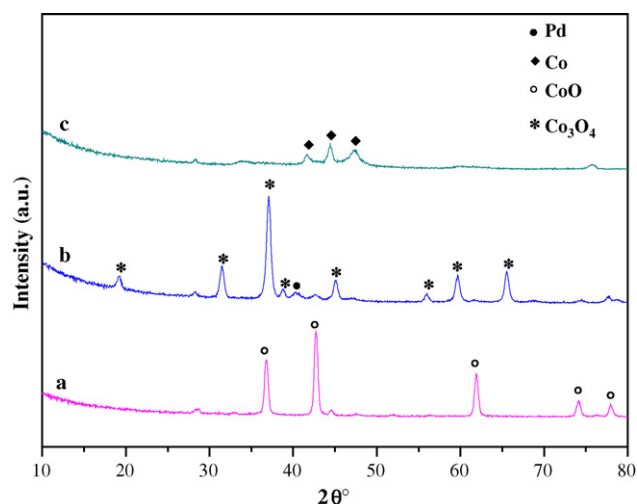
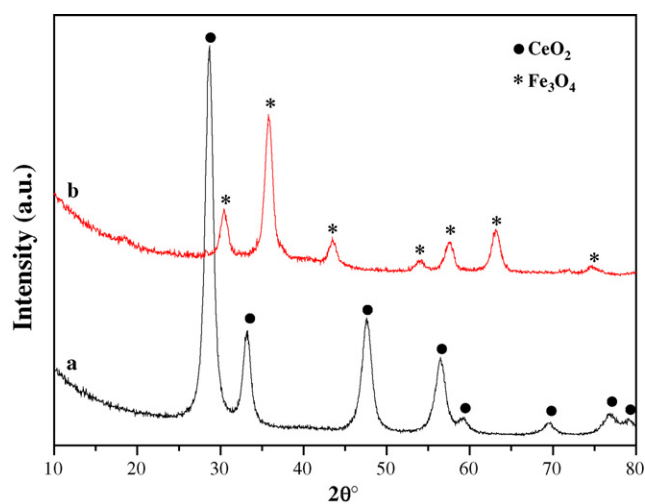**Fig. 5.** XRD patterns of the CoO support and Pd/CoO samples: (a) CoO; (b) Pd/Co$_3$O$_4$; (c) PdCo used.

Fig. 7. XRD patterns of CeO$_2$ and Fe$_2$O$_3$ supported palladium samples: (a) PdCe and (b) PdFe.
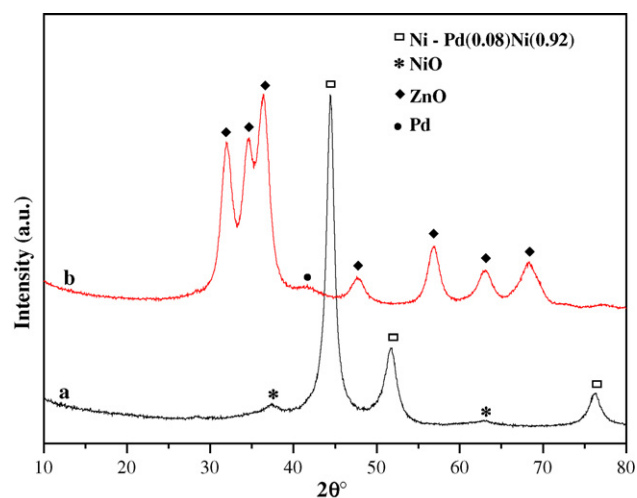

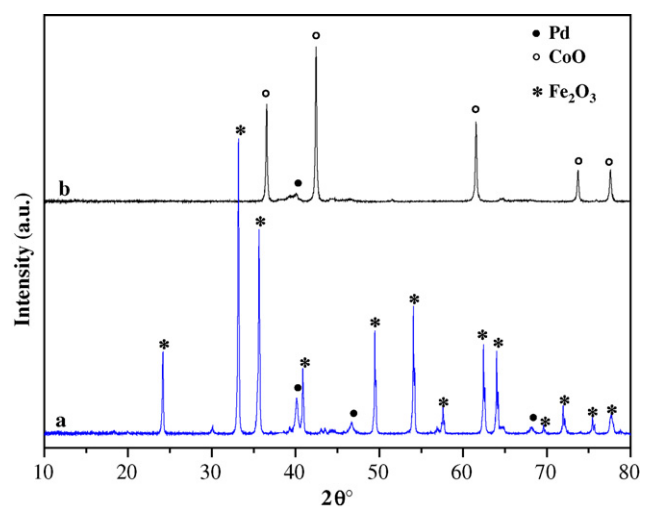**Fig. 6.** XRD patterns of NiO and ZnO supported palladium samples: (a) PdNi and (b) PdZn.

Fig. 8. XRD patterns of CoO and Fe$_2$O$_3$ supported palladium samples, prepared by impregnation: (a) PdFeI and (b) PdCoI.

The absence, on some XRD spectra of co-precipitated catalysts, of any palladium pattern appears an odd, although evident, result. However the co-precipitation technique, used for the catalysts preparation, may influence, in our opinion, the growth of palladium crystallites probably embedded inside the support structure. On the basis of these, TEM an TPR observations we may hypothe-

size that an intimate contact between Pd particles and the support or its metal reduced particles, occurring already in the first stage of their formation, leads to a strong Pd–support (metal) interaction, that hinders crystallization and crystal growth of Pd particles.

Table 3
XPS data of co-precipitated palladium catalysts.

| Catalyst	BE (eV)							
	Pd 3d$_{5/2}$	Co 2p$_{3/2}$	Ni 2p$_{3/2}$	Zn 2p$_{3/2}$	Fe 2p$_{3/2}$	Fe 2p$_{3/2}$ satellite	Fe 2p$_{1/2}$	O 1s
PdCo[a]	337.2	781.5						531.4
Pd/Co$_3$O$_4$ [b]	336.2	781.0						530.1 (15.2%), 531.4 (65.2%), 532.7 (19.6%)
PdNi[a]	337.2		855.9					531.3
PdNi[b]	335.7		854.6					529.2 (35.9%), 530.7 (44.8%), 532.2 (19.3%)
PdZn[a]	337.0			1021.7				531.6
PdZn[b]	334.9			1021.8				529.2 (6.5%), 530.4 (65.6%), 532.1 (27.9%)
PdFe[a]	337.6				710.9	718.8	724.4	530.0 (36.1%), 531.4 (63.9%)
PdFe[b]	335.2				710.9		724.4	529.7 (66.8%), 531.2 (25.8%), 532.6 (7.4%)
PdCe[a]	337.0							529.2 (82.7%), 531.8 (17.3%)
PdCe[b]	336.7							529.1 (49.3%), 530.5 (33.0%), 532.3 (17.7%)

[a] Unreduced.
[b] Reduced at 473 K.
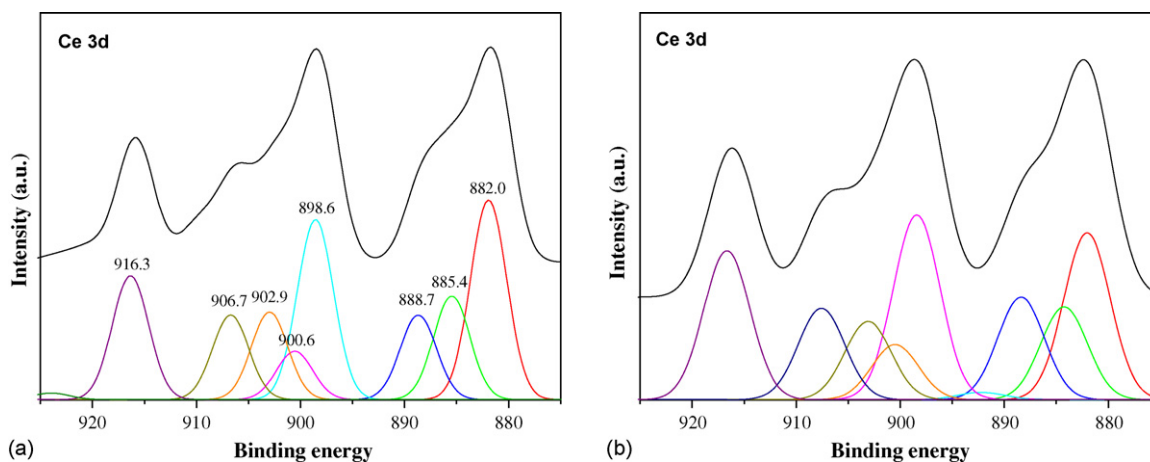
Fig. 9. XPS spectra of PdCe samples: (a) unreduced PdCe and (b) reduced PdCe.

### 3.1.5. X-ray photoelectron spectroscopy (XPS) measurements

Binding energy values for unreduced and reduced catalysts, prepared by co-precipitation, are summarized in Table 3. The XPS spectrum of the fresh Pd/CoO sample exhibits a Co $2p_{3/2}$ peak at 781.5 eV and a strong shake-up satellite shoulder at around 786.3 eV, both indicative of the presence of Co^{2+} species [36]. The Co 2p spectrum of the sample calcined at 773 K and reduced at 473 K evidences a Co $2p_{3/2}$ peak at 781 eV and a very low intensity satellite. The intensity of the shake-up satellite shoulder associated with the Co $2p_{3/2}$ can be used for the identification of the different Co species on the catalyst surface [21,37]. The presence of a very weak satellite peak suggests the presence of Co_3O_4 particles and Co^{2+} surface species.

The XPS spectrum of the unreduced Pd/NiO specimen exhibits a Ni $2p_{3/2}$ band at 855.9 eV with a shake-up feature at 861.1 eV, typical of Ni^{2+} species [38–40]. The same peak shifts at lower binding energy for the reduced sample (854.6 eV). After deconvolution a low intensity peak at 852.5 eV is also detected and attributed to Ni° species [38–41].

Zn $2p_{3/2}$ spectra of reduced and unreduced Pd/ZnO samples are nearly identical and display a peak at about 1021.7 eV and this is in good agreement with the binding energy value of ZnO reported in literature [42,43].

Values of 724.4 eV (Fe $2p_{1/2}$) and 710.9 eV (Fe $2p_{3/2}$) were detected for both unreduced and reduced PdFe specimens (Table 3). Furthermore the absence of the satellite peak at 718.8 eV on the reduced sample suggests, as expected, a magnetite structure, whereas its presence on the unreduced one indicates that of haematite [44,45]. The Ce 3d core level photoemission spectra for the PdCe samples are reported in Fig. 9 and show the typical multiplet structure found for the fully oxidized CeO_2 [46,47]. The presence of five peaks assigned to Ce^{4+} is clearly detected in both unreduced and reduced PdCe samples spectra: three of them are more intense and characterize the Ce $3d_{5/2}$ (BE ~ 882.0 eV, BE ~ 898.6 eV) and Ce $3d_{3/2}$ (BE ~ 916.3 eV) levels. The other two are shoulder and correspond to associated weak satellite peaks (BE ~ 888.7 eV for Ce $3d_{5/2}$ and BE ~ 906.7 eV for Ce $3d_{3/2}$) [48,49]. Moreover, the presence of surface Ce^{3+} on both samples is observed after deconvolution of the experimental spectra. Ce^{3+} has been fitted with two peaks at BE ~ 885.4 eV and BE ~ 902.9 eV, characterizing both Ce $3d_{5/2}$ and Ce $3d_{3/2}$ contributions, respectively.

Data of O 1s XPS spectra for the catalysts are also reported in Table 3. In all cases the O 1s peak is complex. For the unreduced PdCo, PdNi and PdZn samples a symmetric peak at about 531.4 eV is observed and assigned to surface hydroxyl (OH$^-$) and/or carbonate (CO_3^{2-}) species [41,50,51]. Formation of these species is probably
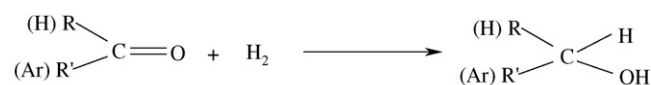
R, R' = alkyl group; Ar = aryl group

Scheme 1. Reduction of carbonyl compounds.

due to the preparation method used. Moreover two components for unreduced Pd/Fe_2O_3 and Pd/CeO_2 samples are obtained, after deconvolution of the O 1s peak: the major with BE at 530.0 eV (529.2 for Pd/CeO_2) is assigned to lattice oxygen (O^{2-}) in the metal oxides, the other one is located at 531.4 eV (531.8 eV for Pd/CeO_2). The deconvolution of O 1s spectra of all reduced catalysts exhibits in addition to the lattice (at 529.1–530.4 eV BE) and non-lattice oxygen (at 530.5–531.8 eV BE) a third peak above 532 eV. It is possible to observe that after reduction the peak assigned to OH$^-$/CO$_3^{2-}$ widely decreases. The relative content of the different kinds of oxygen in the total surface can be estimated from the relative area of these peaks and the results are also included in Table 3.

The Pd $3d_{5/2}$ binding energy is very peculiar (Table 3) and, in unreduced samples, is found in the range between 337.0 and 337.6 eV. It has been reported that in PdO the binding energy value is at 336.8 eV whereas, on our specimens, it is, in some way, at a higher energy level suggesting, in this case, that Pd^{2+} is more cationic than in PdO [52,53]. Usually this phenomenon is thought to derive from a strong metal–support interaction [54]. On reduced samples, binding energy values are between 334.9 and 335.7 eV, as expected for Pd° particles [51,55]. However values of 336.2 and 336.7 eV were found, respectively for Pd/Co_3O_4 (calcined at 773 K) and PdCe samples, after reduction at 473 K. In this case possible $Pd^{\delta+}$ like species ($0 < \delta < 2$) may be present and, in the case of PdCe, probably deriving from a PdOCe interaction as already reported in literature [56,57].

3.2. Hydrogenation reactions

The reduction of carbonyl compounds was carried out in ethanol solution, at 323 K and 0.1 MPa H_2 pressure in a reaction pathway as reported in Scheme 1.

Initial reaction rates, r_i, expressed as moles of substrates/grams of palladium per second, are reported in Tables 4 and 5. A typical composition against time plot is shown in Fig. 10. It clearly appears that, in aldehydes series, aromatic derivatives are easily hydrogenated and undergo a further reduction of the produced alcohol

Table 4
Activity of supported Pd catalysts in aldehydes hydrogenation at 323 K and 0.1 MPa H_2 pressure, using ethanol as solvent.

Catalyst	r_i ($\times 10^5$ mol$_{sub}$/g$_{Pd}$ s)				
	Propanal[a]	Pentanal	Hexanal	3-Phenylpropanal	Benzaldehyde
PdCo	4.6	23.0	17.4	4.3	24.6
PdNi	2.4	10.3	7.8	2.6	13.1
PdZn	0.5	1.3	–	–	2.9
PdFe	4.1	11.2	8.8	3.2	27.7
PdCe	1.0	3.3	1.4	0.2	9.7
PdCoI		Very slow			6.5
PdFeI		Very slow			23.9

[a] Values at 303 K.

Table 5
Activity of co-precipitated Pd catalysts in ketones hydrogenation at 323 K and 0.1 MPa H_2 pressure, using ethanol as solvent.

Catalyst	r_i ($\times 10^5$ mol$_{sub}$/g$_{Pd}$ s)			
	Pentan-2-one	Pentan-3-one	Cyclohexanone	1-Phenylethanone
PdCo	1.6	6.7	23.1	6.5
PdNi	0.3	0.4	10.8	2.2
PdZn	–	–	0.4	1.6
PdFe	0.2	–	3.9	19.0
PdCe	–	0.5	15.8	8.3

to hydrocarbons. Conversely, aliphatic aldehydes are hydrogenated by PdCo, PdNi, PdFe and PdCe and the rate increases in the following order: pentanal > hexanal > 3-phenylpropanal, as normally expected when a rate dependence on the chain length occurs. The PdZn catalyst shows a weak activity and only for pentanal a small r_i value was possible to be calculated. Propanal is also hydrogenated; however, the reaction was carried out at 303 K, on account of the low aldehyde boiling temperature (319 K), and the relative rate is also included. Again PdZn is much less active. In ketones series, the aromatic 1-phenylethanone is easily hydrogenated. On PdCo and PdNi aliphatic ketones show the following behaviour: the most reactive is cyclohexanone and the symmetric pentan-3-one is more active than pentan-2-one. PdFe and PdCe show a good activity only towards cyclohexanone and are pratically inactive towards the other ketones. PdZn is only poorly active towards cyclohexanone. Experiments carried out, using Pd/Co$_3$O$_4$ as catalyst, evidence a very slow reaction in aliphatic aldehydes hydrogenation.

Furthermore, the pentanal hydrogenation, carried out in presence of a CoO sample, reduced at a temperature allowing partial reduction of Co^{2+} (700 K) and then containing metallic Co, does not afford any alcohol formatio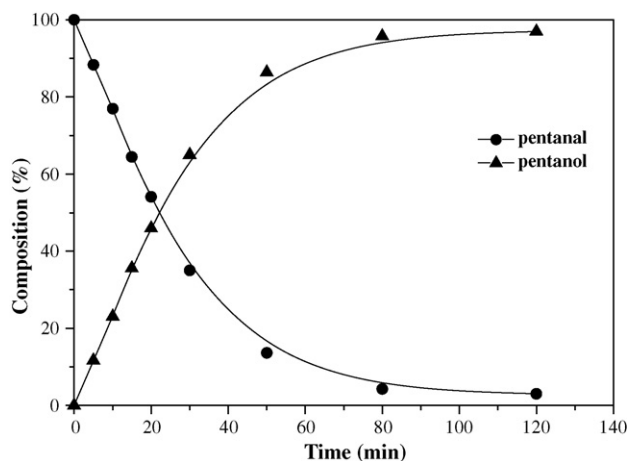n, thus excluding participation of the supported metal to the reaction. The same experiment was also repeated by using NiO, previously reduced at 723 K, and again no alcohol was formed. Impregnated catalysts, PdCoI and PdFeI, afford an easy reduction of benzaldehyde and a very slow reduction of pentanal.
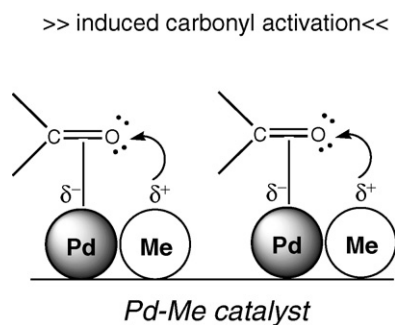
4. Discussion

The reported results, considered all together, allow an useful comparison to investigate the intimate mechanism of carbonyl compounds hydrogenation.

So far palladium particles, supported on common carriers, were found to be active in the hydrogenation of aromatic aldehydes or ketones but inefficient towards aliphatic carbonyls reduction [12,15]. This different behaviour depends, in our opinion, on the Δ energy difference between π and π^* orbitals (small in aromatic derivatives and higher in aliphatic ones) [58]. This trend is confirmed by the U, V, λ values, related to the $\pi \rightarrow \pi^*$ gap of carbonyls, which are higher in aromatic aldehydes (249 nm for benzaldehyde) and much lower ($\sim$185 nm in aliphatic aldehydes or ketones) in aliphatic carbonyls.

It was already pointed out that the main attractive effect, in the adsorption of aldehydes on a metal surface, is the back donation of electrons from the metal orbitals into the π^*_{CO} [12]. When this latter is shifted down, the interaction is easier and the adsorption occurs. This is, indeed, what happens with aromatic aldehydes or ketones, thus easily hydrogenated.

The observed carbonyl reduction of aliphatic aldehydes or ketones with our co-precipitated samples can be explained with an insight remark on the electronic peculiarities of the catalysts mainly deriving from the Pd–support or Pd–metal interaction. The reactivity cannot be attributed, in fact, only to a metal particles size effect: catalysts having a similar particles diameter (PdZn and PdFe) show a very different reactivity. On the other hand, the variation observed in surface area values (see Table 1) surely affects the reactivity but, on itself, does not explain our results: although PdFe displays the highest surface area, it was found less active than PdCo and again PdNi and PdZn, having very different activity, show similar values of BET surface area. Furthermore, whereas the large difference in BET values between co-precipitated and impregnated samples could explain the remarkable variation in hydrogenation activity observed in the aliphatic aldehydes series, however it does

Fig. 10. Composition–time plot of the hydrogenation reaction of pentanal over PdCo at 323 K and 0.1 MPa H_2 pressure, using ethanol as solvent.

>> induced carbonyl activation<<

Scheme 2. Induced carbonyl interaction of aliphatic aldehydes or ketones with PdMe catalysts.

not fit completely the aromatic series data. Therefore, electronic effects play an important role in driving the observed activity.

For clearness sake we prefer to discuss separately results referring to PdCo, PdNi and PdZn from those concerning PdFe and PdCe for their different electronic peculiarities.

4.1. Hydrogenation promoted by PdCo, PdNi and PdZn catalysts

Aliphatic aldehydes or ketones are extensively reduced by PdCo or PdNi, whereas only pentanal and propanal (very slowly) and, in a few extent, cyclohexanone, react with H_2 in presence of PdZn. The observed carbonyl reduction appears to be mainly related to the amount of bimetallic PdMe "ensembles" formation (as confirmed by TPR, XRD and XPS measurements). Accordingly, when we use the impregnated Pd/CoO only a very slow reaction occurs with pentanal. The TPR profile (Fig. 3) clearly indicates, in the last case, the absence of any PdCo species formation and therefore a scarce metal–support interaction. On the other hand, it is perfectly understandable the easy reactivity of the aromatic aldehyde with the PdCoI catalyst.

The reason why bimetallic particles or alloys favour the reactivity of aliphatic carbonyl compounds should be mainly found on the change of the electronic properties of palladium promoted by the second metal. XANES and EXAFS studies have so far demonstrated that on PdCo [21] and PtCo [59] species a shift of electrons from Co to Pd (Pt) occurs. On this basis it may be assumed that, on the surface, clusters formed by both Pd(0) and Co(Ni)(0) atoms, in intimate contact, may favour an electronic transfer from Co(Ni) to palladium, leading to a negative charge on Pd and a positive one on Co(Ni).

As a consequence, the d orbitals of Pd at the Fermi level should be shifted upward, thus favouring the back donation of electrons to the π^*_{CO}. The hydrogenation process could be also helped by the positively charged Co or Ni neighbours acting as electron-attractors towards the carbonyl oxygen cloud (Scheme 2).

4.2. Hydrogenation promoted by PdFe and PdCe catalysts

XPS spectra of PdCe and PdFe catalysts indicate the presence of both Fe^{3+}/Fe^{2+} and Ce^{4+}/Ce^{3+} couples on the surface. Besides, TPR profiles are similar and both propose an easy reduction of Fe^{3+} and surface Ce^{4+} to Fe^{2+} and Ce^{3+}, respectively, in presence of palladium particles. On the light of our structural evidences, in absence of any alloy on the surface, the most convincing picture, that we can draw for reduction of aliphatic aldehydes, in our opinion, implies an oxidative approach by Fe^{3+} or Ce^{4+} on the oxygen moiety of a carbonyl molecule, their reduction to Fe^{2+} and Ce^{3+}, respectively and the subsequent lowering of the π^*_{CO} favouring the activation of the carbonyl bond on the Pd surface. Accordingly a very slow reaction occurs on the impregnated Pd/Fe$_2$O$_3$ using

pentanal as substrate with respect to the analogous co-precipitated sample.

In other words, the main difference between the behaviour of Pd and that of Pt, Ru, Rh and other metals rests on the assumption that, on the majority of platinum metals series the strength of common Lewis acids is sufficient to induce an "electrophilic C=O activation" whereas, when supported palladium is used, the peculiarity of its electronic properties [12] implies the necessity of a stronger redox couple presence.

5. Conclusions

The results reported indicate that the behaviour of supported palladium catalysts, in the hydrogenation of carbonyl compounds, can be modified using an appropriate preparation method (co-precipitation technique) and a more fitting metal oxide as support. So far literature reports indicated that H_2 reduction of aliphatic aldehydes and ketones is a very difficult reaction to occur with Pd systems. Our data suggest that it can be easily performed mainly by changing the electronic properties of palladium, allowing formation, during the activation procedure at 473 K, of bimetallic particles with PdCo or PdZn in less extent, or of an alloy in the case of a PdNi system.

A comparison between the aromatic and aliphatic carbonyl reactivity suggests that the first is easily activated on a palladium surface since the Δ value π–π^* is appreciably shorter than that of the aliphatic one (reduction of aromatic carbonyls is easy to be carried out with common palladium catalysts). However, if the energy value of the d band at the Fermi level of palladium is increased, population of π^* orbitals and then activation of the C=O bond can occur. This is indeed what happens when bimetallic ensembles or an alloy are formed, during the activation procedure, in PdCo, PdZn (in less extent) and PdNi catalysts. Similarly PdFe and PdCe catalysts form suitable redox couples, Fe^{3+}/Fe^{2+} or Ce^{4+}/Ce^{3+} on the palladium surface; interaction of Fe^{3+} or Ce^{4+} with the oxygen moiety of the carbonyl lowers the π^* energy level and favours aliphatic aldehydes activation. A comparison with the reactivity of Pd/CoO and Pd/Fe$_2$O$_3$, prepared by impregnation, supports this conclusion.

References

[1] D. Gallezot, D. Richard, Catal. Rev. -Sci. Eng. 40 (1998) 81–126.
[2] U.K. Singh, M.A. Vannice, J. Catal. 199 (2001) 73–84.
[3] P. Reyes, H. Rojas, G. Pecchi, J.L.G. Fierro, J. Mol. Catal. A: Chem. 179 (2002) 293–299.
[4] P. Mäki-Arvela, J. Hájek, T. Salmi, D.Yu. Murzin, Appl. Catal. A: Gen. 292 (2005) 1–49.
[5] Z. Poltarzewski, S. Galvagno, R. Pietropaolo, P. Staiti, J. Catal. 102 (1986) 190–198.
[6] S. Galvagno, A. Donato, G. Neri, R. Pietropaolo, Catal. Lett. 8 (1991) 9–14.
[7] V. Ponec, Appl. Catal. A: Gen. 149 (1997) 27–48.
[8] T.B.L.W. Marinelli, V. Ponec, J. Catal. 156 (1995) 51–59.
[9] M.A. Aramendía, V. Borau, C. Jiménez, J.M. Marinas, A. Porras, F.J. Urbano, J. Catal. 172 (1997) 46–54.
[10] L. Sordelli, R. Psaro, G. Vlaic, A. Cepparo, S. Recchia, C. Dossi, A. Fusi, R. Zanoni, J. Catal. 182 (1999) 186–198.
[11] S. Sato, R. Takahashi, T. Sodesawa, M. Koubata, Appl. Catal. A: Gen. 284 (2005) 247–251.
[12] F. Delbecq, P. Sautet, J. Catal. 152 (1995) 217–236.
[13] V. Ponec, G.C. Bond, Catalysis by Metals and Alloys, Series Surf. Sci. and Catal., 96, Elsevier, Amsterdam, 1995.
[14] F. Pinna, F. Menegazzo, M. Signoretto, P. Canton, G. Fagherazzi, N. Pernicone, Appl. Catal. A: Gen. 219 (2001) 195–200.
[15] H.-U. Blaser, A. Indolese, A. Schnyder, H. Steiner, M. Studer, J. Mol. Catal. A: Chem. 173 (2001) 3–18.
[16] J.-Q. Yu, H.C. Wu, C. Ramarao, J.B. Spencer, S.V. Ley, Chem. Commun. (2003) 678–679.
[17] M.J. Gracia, J.M. Campelo, E. Losada, R. Luque, J.M. Marinas, A.A. Romero, Org. Biomol. Chem. 7 (2009) 4821–4824.
[18] G. Neri, G. Rizzo, L. De Luca, A. Donato, M.G. Musolino, R. Pietropaolo, React. Kinet. Catal. Lett. 93 (2008) 193–202.
[19] G. Neri, G. Rizzo, L. De Luca, A. Donato, M.G. Musolino, R. Pietropaolo, Appl. Catal. A: Gen. 356 (2009) 113–120.

[20] F.B. Noronha, M. Schmal, R. Fréty, G. Bergeret, B. Moraweck, J. Catal. 186 (1999) 20–30.
[21] F.B. Noronha, M. Schmal, B. Moraweck, P. Delichère, M. Brun, F. Villain, R. Fréty, J. Phys. Chem. B 104 (2000) 5478–5485.
[22] C. Montes de Correa, F. Córdoba Castrillón, J. Mol. Catal. A: Chem. 228 (2005) 267–273.
[23] M.G. Musolino, G. Apa, A. Donato, R. Pietropaolo, F. Frusteri, Appl. Catal. A: Gen. 325 (2007) 112–120.
[24] Y.-H. Chin, R. Dagle, J. Hu, A.C. Dohnalkova, Y. Wang, Catal. Today 77 (2002) 79–88.
[25] A. Benedetti, G. Fagherazzi, F. Pinna, G. Rampazzo, M. Selva, G. Strukul, Catal. Lett. 10 (1991) 215–223.
[26] G. Neri, A.M. Visco, S. Galvagno, A. Donato, M. Panzalorto, Thermochim. Acta 329 (1999) 39–46.
[27] A. Basińska, T.P. Maniecki, W.K. Jóźwiak, React. Kinet. Catal. Lett. 89 (2006) 319–324.
[28] A. Basińska, W.K. Jóźwiak, J. Góralski, F. Domka, Appl. Catal. A: Gen. 190 (2000) 107–115.
[29] C. Milone, R. Ingoglia, L. Schipilliti, C. Crisafulli, G. Neri, S. Galvagno, J. Catal. 236 (2005) 80–90.
[30] H. Zhu, Z. Qin, W. Shan, W. Shen, J. Wang, J. Catal. 225 (2004) 267–277.
[31] V. Ferrer, A. Moronta, J. Sánchez, R. Solano, S. Bernal, D. Finol, Catal. Today 107–108 (2005) 487–492.
[32] S.A.A. Mansour, Mater. Chem. Phys. 36 (1994) 309–316.
[33] B. Ernst, A. Bensaddik, L. Hilarie, P. Chaumette, A. Kiennemann, Catal. Today 39 (1998) 329–341.
[34] A. Infantes-Molina, J. Mérida-Robles, E. Rodríguez-Castellón, J.L.G. Fierro, A. Jiménez-López, Appl. Catal. A: Gen. 341 (2008) 35–42.
[35] A. Infantes-Molina, J. Mérida-Robles, E. Rodríguez-Castellón, B. Pawelec, J.L.G. Fierro, A. Jiménez-López, Appl. Catal. A: Gen. 286 (2005) 239–248.
[36] T.J. Chuang, C.R. Brundle, D.W. Rice, Surf. Sci. 59 (1976) 413–429.
[37] A.M. Venezia, R. Murania, G. Pantaleo, V. la Parola, S. Sciré, G. Deganello, Appl. Catal. A: Gen. 353 (2009) 296–304.
[38] T.L. Barr, J. Phys. Chem. 82 (1978) 1801–1810.
[39] A.P. Grosvenor, M.C. Biesinger, R.St.C. Smart, N.S. McIntyre, Surf. Sci. 600 (2006) 1771–1779.
[40] K. Hadjiivanov, M. Mihaylov, D. Klissurski, P. Stefanov, N. Abadjieva, E. Vassileva, L. Mintchev, J. Catal. 185 (1999) 314–323.
[41] J.-G. Kim, D.L. Pugmire, D. Battaglia, M.A. Langell, Appl. Surf. Sci. 165 (2000) 70–84.
[42] J.F. Moulder, W.F. Stickle, P.E. Sobol, K.D. Bomben, in: J. Chastain (Ed.), Handbook of X-ray Photoelectron Spectroscopy, Perkin-Elmer, Eden Prairie, MN, 1992.
[43] K. Dumbuya, R. Deneke, H.-P. Steinrück, Appl. Catal. A: Gen. 348 (2008) 209–213.
[44] M. Muhler, R. Schlögl, G. Ertl, J. Catal. 138 (1992) 413–444.
[45] T. Yamashita, P. Hayes, Appl. Surf. Sci. 254 (2008) 2441–2449.
[46] H. Idriss, C. Diagne, J.P. Hindermann, A. Kiennemann, M.A. Barteau, J. Catal. 155 (1995) 219–237.
[47] F. Larachi, J. Pierre, A. Adnot, A. Bernis, Appl. Surf. Sci. 195 (2002) 236–250.
[48] G. Praline, B.E. Koel, R.L. Hance, H.I. Lee, J.M. White, J. Electron Spectrosc. Relat. Phenom. 21 (1980) 31–46.
[49] E. Paparazzo, Surf. Sci. Lett. 234 (1990) L253–L258.
[50] L.G. Tejuca, A.T. Bell, J.L.G. Fierro, M.A. Pena, Appl. Surf. Sci. 31 (1988) 301–316.
[51] M.L. Cubeiro, J.L.G. Fierro, J. Catal. 179 (1998) 150–162.
[52] M. Burn, A. Berthet, J.C. Bertolini, J. Electron Spectrosc. Relat. Phenom. 104 (1999) 55–60.
[53] W.-J. Shen, Y. Matsumura, J. Mol. Catal. A: Chem. 153 (2000) 165–168.
[54] K. Sun, W. Lu, M. Wang, X. Xu, Appl. Catal. A: Gen. 268 (2004) 107–113.
[55] N. Iwasa, S. Masuda, N. Ogawa, N. Takezawa, Appl. Catal. A: Gen. 125 (1995) 145–157.
[56] W.-J. Shen, Y. Matsumura, Phys. Chem. Chem. Phys. 2 (2000) 1519.
[57] Y. Matsumura, W.-J. Shen, Y. Ichihashi, M. Okumura, J. Catal. 197 (2001) 267–272.
[58] J. Kneisher, Z. Zhon, Int. J. Quantum Chem. 49 (1994) 309–320.
[59] N.M. Bertero, A.F. Trasarti, B. Moraweck, A. Borgna, A.J. Marchi, Appl. Catal. A: Gen. 358 (2009) 32–41.